

FINITE ELEMENT METHODS FOR NONLINEAR
ELASTOSTATIC PROBLEMS IN RUBBER ELASTICITY

J. T. Oden, E. B. Becker, T. H. Miller, T. Endo, and E. B. Pires
The University of Texas at Austin

ABSTRACT

This paper outlines a number of finite element methods for the analysis of nonlinear problems in rubber elasticity. Several different finite element schemes are discussed. These include the augmented Lagrangian method, continuation or incremental loading methods, and associated Riks-type methods which have the capability of incorporating limit point behavior and bifurcations. Algorithms for the analysis of limit point behavior and bifurcations are described and the results of several numerical experiments are presented. In addition, a brief survey of some recent work on modelling contact and friction in elasticity problems is given. These results pertain to the use of new nonlocal and nonlinear friction laws.

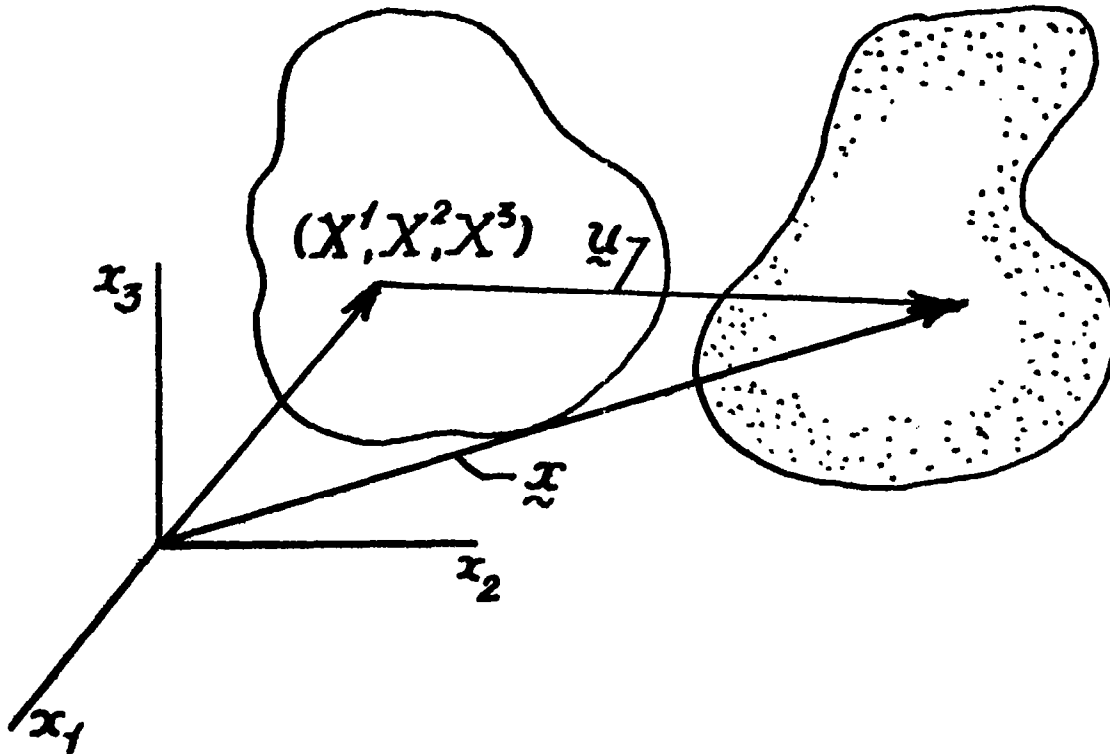
OUTLINE

1. PRELIMINARIES AND NOTATION
2. FINITE ELEMENT MODELS
3. ALGORITHMS
4. NUMERICAL EXPERIMENTS
5. FRICTION MODELS
6. NUMERICAL RESULTS

PRELIMINARIES AND NOTATIONS

KINEMATICS

The usual notation in finite elasticity is employed: \underline{u} is the displacement vector, \underline{x} is the position of a particle in the current configuration whose position was \underline{X} in the reference configuration, \underline{F} is the deformation gradient. These quantities are illustrated in the figure below.



\underline{u} = DISPLACEMENT VECTOR

$$\underline{u} = \underline{x} - \underline{X}$$

\underline{F} = DEFORMATION GRADIENT

$$\underline{F} = \nabla(\underline{X} + \underline{u}) ; F_{\alpha i} = \frac{\partial}{\partial X^\alpha} (X^i + u^i)$$

HOMOGENEOUS, ISOTROPIC

HYPERELASTIC MATERIAL

We begin with a study of equilibrium problems in finite elasticity. It is assumed that the materials involved are hyperelastic, isotropic, and homogeneous. Therefore, they are characterized by a strain energy function W which is given as a function of invariants of the deformation tensor \underline{C} . These problems are complicated by the fact that nonconvex constraints must be enforced. For compressible materials the constraint manifests itself in the condition that $J(\underline{u}) = \det \underline{F} > 0$ while for incompressible materials $J(\underline{u}) = 1$.

$$W = \hat{W}(I_1, I_2, J) = \text{STRAIN ENERGY PER UNIT VOLUME}$$

$$I_1 = \text{TRACE } \underline{C}$$

$$I_2 = \frac{1}{2} (\text{TRACE } \underline{C})^2 - \frac{1}{2} \text{TRACE } \underline{C}^2$$

$$J = \sqrt{I_3} = \det \underline{F} \quad \underline{C} = \underline{F}^T \underline{F}$$

COMPRESSIBLE MATERIALS

$$J(\underline{u}) = \det \underline{F} > 0$$

INCOMPRESSIBLE MATERIALS

$$J(\underline{u}) = 1$$

SOME CONDITIONS ON THE FORM OF W

Some conditions on the form of the energy W are presented below. In addition to the fact that the energy must be form invariant under changes of the spatial frame of reference, other conditions must be enforced if one expects a well-behaved solution. Three of these are listed below:

1. COERCIVITY:

$$W(\underline{u}) = \hat{W}(I_1(\underline{u}), I_2(\underline{u}), J(\underline{u}))$$

$$W(\underline{u}) \rightarrow +\infty \text{ as } \|\nabla \underline{u}\| \rightarrow +\infty$$

2. SINGULAR BEHAVIOR:

$$W(\underline{u}) \rightarrow +\infty$$

$$\text{as } \det F \rightarrow 0^+$$

$$\left| \frac{\partial W}{\partial F} \right| \rightarrow +\infty$$

3. QUASICONVEXITY:

$$\left\langle \frac{\partial^2 W(\underline{u})}{\partial F_{i\alpha} \partial F_{j\beta}} \right\rangle \lambda_{i\alpha} \lambda_{j\beta} \geq 0$$

$$\forall \lambda_{i\alpha}, \mu_{j\beta} \in \mathbb{R}^3$$

INCOMPRESSIBLE AND NEARLY INCOMPRESSIBLE MATERIALS

Two basic classes of methods are employed here to handle compressible and nearly incompressible materials: Lagrange-multiplier methods (mixed methods), in which the incompressibility constraint $h(J) = 0$ is accounted for using Lagrange multipliers and penalty methods in which the total potential energy functional Π is penalized by the addition of a positive semi-definite, generally convex penalty functional.

INCOMPRESSIBILITY CONSTRAINT

$$h(J) = 0$$

$$h(J) = J - 1, J^2 - 1, (J - 1)^2, -\ln J, \text{ etc.}$$

$$W = \tilde{W}(I_1, I_2) - p h(J)$$

$$p = \text{Lagrange Mult.} \approx \text{Hydrostatic Pressure}$$

PENALTY TERMS

$$\begin{aligned} \Pi(\underline{u}) &= \int_{\Omega} W(\underline{u}) dX - f(\underline{u}, \underline{v}) \\ &\quad + \epsilon^{-1} \int_{\Omega} g(J(\underline{u})) dX \end{aligned}$$

$$g(J) \geq 0 \quad g(J) = 0 \leftrightarrow J = 1$$

EQUILIBRIUM CONDITIONS

The finite elements employed are based on various alternative statements of equilibrium conditions for elastic bodies:

1) ENERGY FORMULATION

$$\begin{aligned} \pi(\underline{u}) &= \text{TOTAL POTENTIAL ENERGY} \\ &= \int_{\Omega} W(\underline{u}) dX + f(\underline{u}, \underline{v}) \\ f(\underline{u}, \underline{v}) &= \int_{\Omega} f(\underline{u}) \cdot \underline{v} dX + \int_{\Gamma_2} \underline{t}(\underline{u}) \cdot \underline{v} ds \end{aligned}$$

$$\begin{aligned} \pi(\underline{u}) &\leq \pi(\underline{v}) \text{ for all } \underline{v} \text{ in} \\ K &= \{ \underline{v} : \int_{\Omega} W(\underline{v}) dX < \infty ; \\ &\quad \underline{v} = \underline{0} \text{ on } \Gamma_1 ; \det \nabla \underline{v} \geq 0 \text{ or } = 1 \} \end{aligned}$$

2) AUGMENTED LAGRANGE

$$\begin{aligned} L(\underline{u}, \underline{F}, \underline{\lambda}) &= \pi(\underline{u}) + \frac{\epsilon}{2} \int_{\Omega} |\nabla \underline{u} - \underline{F}|^2 dX \\ &\quad + \int_{\Omega} \underline{\lambda} : (\nabla \underline{u} - \underline{F}) dX \\ L: \underline{v} \times (\underline{G} : \det \underline{G} = 1) \times (\dots)^* \end{aligned}$$

The augmented Lagrange method combines features of both penalty and Lagrange-multiplier schemes. The incompressibility constraint can be satisfied a priori in a straightforward manner for Mooney-Rivlin materials, with the result that the method is extremely fast and efficient when used in conjunction with, e.g., Uzawa's method (ref 1). (See equation.)

3. VIRTUAL WORK I

$$\begin{aligned} \int_{\Omega} v_{i,\alpha} \frac{\partial W(\underline{u})}{\partial u_{i,\alpha}} dX - \int_{\Omega} \rho \frac{\partial h}{\partial J} \cdot \frac{\partial J}{\partial u_{i,\alpha}} \cdot v_{i,\alpha} dX \\ = f(\underline{u}, \underline{v}) \text{ for all } \underline{v} \text{ in } \underline{V} \\ \int_{\Omega} q h(J(\underline{u})) dX = 0 \text{ for all } q \text{ in } Q \end{aligned}$$

4. VIRTUAL WORK II

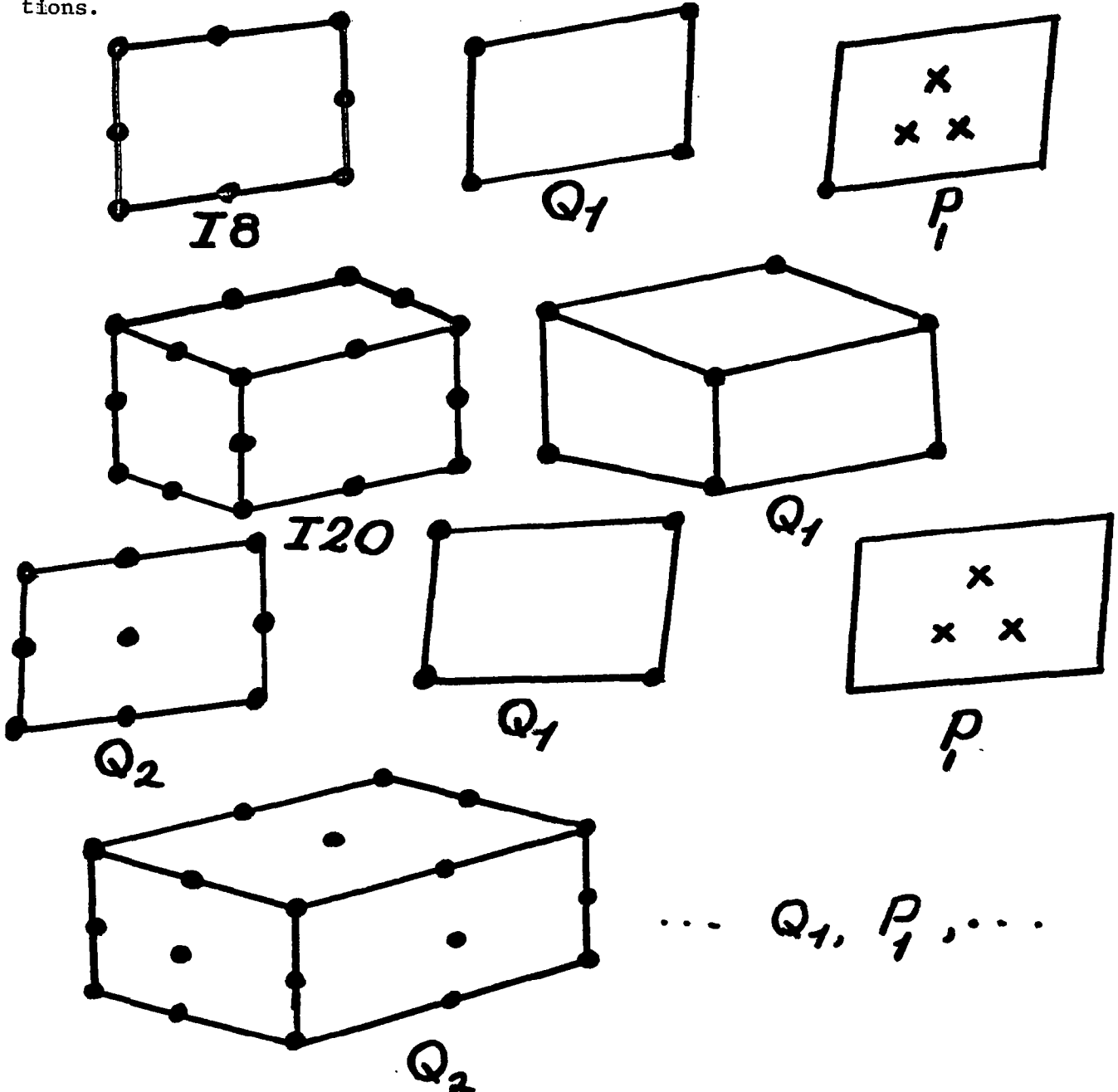
$$\begin{aligned} \int_{\Omega} \frac{\partial W(\underline{u}_\epsilon)}{\partial u_{i,\alpha}} v_{i,\alpha} dX + \epsilon^{-1} \int_{\Omega} \frac{\partial g}{\partial J} \cdot \frac{\partial J}{\partial u_{i,\alpha}} v_{i,\alpha} dX \\ = f(\underline{u}_\epsilon, X) \text{ for all } \underline{v} \text{ in } \underline{V} \end{aligned}$$

$$p_\epsilon = - \epsilon^{-1} \frac{\partial g(J(\underline{u}_\epsilon))}{\partial J}$$

FINITE ELEMENT METHODS

SOME ELEMENT FAMILIES

The figure below illustrates some of the standard finite element methods employed. Unfortunately, not all of these methods are numerically stable since some may not satisfy the generalized LBB condition of Oden and LeTallec (refs. 2 and 3). This condition is given in the equation on the following page, where Q is the space of Lagrange multipliers, V_h is the space of finite element approximations of displacement, p is the hydrostatic pressure and $||\nabla v^h||_{0,p}$ is an appropriate energy norm on V^h . The existence of a $\beta_h > 0$ independent of mesh size h is necessary for the stability of the mixed and penalty methods, particularly for pressure approximations.



THE GENERALIZED LBB CONDITION

(REFS. 2 AND 3)

$\beta_h(\underline{u}) > 0$ such that

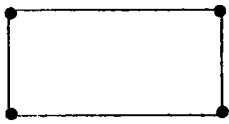
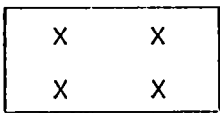

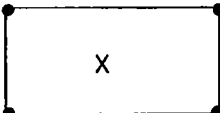

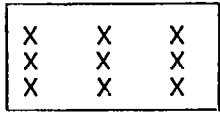
$$\beta_h \|p\|_{Q/\ker \nabla J(\underline{u})} \leq \max_{V_h} \frac{\int_{\Omega} p \frac{\partial J(\underline{u})}{\partial u_{i,\alpha}} v_{i,\alpha}^h dx}{\|\nabla v^h\|_{0,p}}$$

for all p in Q

The numerical stability of mixed- and penalty finite element methods depends upon this condition, and particularly on the behavior of the parameter β_h with the mesh size h .

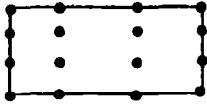
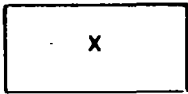
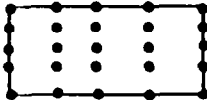
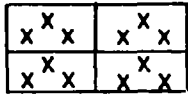
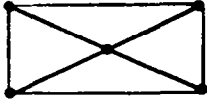
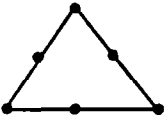
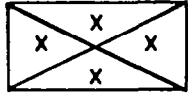
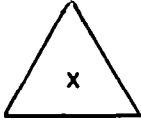
STABILITY RESULTS

Oden and Jacquotte (ref, 4) have recently completed a mathematical analysis of the LBB condition for incompressible viscous flows. Some of these results appear to be directly applicable to the finite elasticity problem. The following table summarizes the behavior of certain finite element methods for these constrained problems. The results generally fall into three categories: the stability parameter β_h is independent of h and the method is stable, β_h is dependent on h and the method is unstable having spurious pressure modes, or the element is "locked", meaning that the penalty parameter ε depends on the mesh size and that the displacements approach 0 as ε tends to zero for a fixed mesh size h .

VELOCITY APPROX.	QUADRATURE RULE (PRESSURE APPROX. Q)		CONVERGENCE RATE
1  Q_1	 Q_2	$O(1)$	LOCKS
2  Q_1	 Q_0	$O(h)$	UNSTABLE
3  $1B$	 Q_2	$O(1)$	LOCKS

VELOCITY APPROX.	PRESSURE		RATE OF CONVERGENCE
4 I8	 Q_1	$O(h)$	UNSTABLE PRESSURE
5 I8	 P_1	$O(h)$	UNSTABLE PRESSURE
6 I8	 Q_0	$O(1)$	SUBOPTIMAL ($O(h)$) IN VELOCITY ERROR IN ENERGY NORM
7 Q_2	 Q_2	$O(1)$	LOCKS FOR SMALL ϵ ; ϵ MUST BE TAKEN AS DEPENDENT ON h

VELOCITY APPROX.	PRESSURE		RATE OF CONVERGENCE
8 Q_2	 Q_1	$O(h)$	UNSTABLE PRESSURE
9 Q_2	 P_1	$O(1)$	OPTIMAL :
10 Q_2	 Q_0	$O(1)$	SUBOPTIMAL ($O(h)$) IN VELOCITY ERROR IN ENERGY NORM
11 Q_3	 Q_2	$O(h)$	UNSTABLE PRESSURE*

VELOCITY APPROX.	PRESSURE		RATE OF CONVERGENCE
12  Q_3	 Q_0	$O(1)$	SUBOPTIMAL ($O(h)$) IN VELOCITY ERROR IN ENERGY NORM*
13  COMPOSITE Q_2/I_8	 COMPOSITE $4 P_1$	$O(1)$	OPTIMAL
14  COMPOSITE $4 P_1$  P_2	 COMPOSITE $4P_0$  $P_0 P_0$	$O(h)$ $O(1)$	UNSTABLE PRESSURE SUBOPTIMAL ($O(h)$) IN VELOCITY ERROR IN ENERGY NORM

ALGORITHMS

Several different algorithms are employed for the analysis of finite elasticity problems. These include the augmented Lagrange/Uzawa methods, continuation (incremental loading) methods, and homotopy methods. In the present paper, augmented Lagrange methods are discussed briefly, but the focus is on the continuation-type methods of, for example, Riks (ref. 5), Keller (ref. 6), Crisfield (ref. 7), and Padovan (ref. 8).

1. AUGUMENTED LAGRANGE/UZAWA

1. EXTREMELY SIMPLE & FAST
2. FOLLOWS STABLE BRANCHES
3. NOT EASILY ADAPTED TO GENERAL MAT'LS

2. CONTINUATION (INCREMENTAL LD'G)

1. RIKS (REF. 5), WEMPNER (REF. 9)
2. KELLER (REF. 6), RHEINBOLT (REF. 10)
3. CRISFIELD (REF. 7), PADOVAN (REF. 8)

3. HOMOTOPY METHODS

$$f(\tilde{x}, \tilde{p}) = 0$$

$$\frac{\partial f(\tilde{x}(s), \tilde{p}(s))}{\partial \tilde{x}} \dot{\tilde{x}} + \frac{\partial f(\tilde{x}(s), \tilde{p}(s))}{\partial \tilde{p}} \dot{\tilde{p}} = 0$$

$$N(\dot{\tilde{x}}(s), \dot{\tilde{p}}(s)) = 0$$

+ ODE SOLVER

AUGUMENTED LAGRANGE METHOD

The augmented Lagrange is a super-fast method.

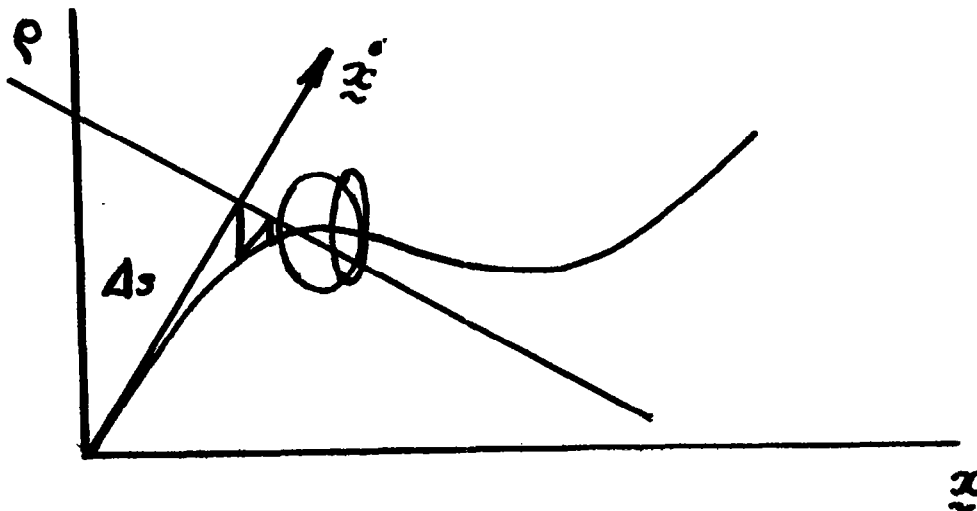
AUGUMENTED LAGRANGE \Rightarrow BLOCK RELAXATION

1. $\tilde{\lambda}^{n+1} = \tilde{\lambda}^n - p (\nabla u^n - \tilde{F}^n)$
2. $L(u_k^n, \tilde{F}_{k+1}^n, \tilde{\lambda}^n) \leq L(u_k^n, \tilde{G}, \tilde{\lambda}^n)$
 | SOLVED EXPLICITLY, $N + 2, 3$ |
3. $\partial_v L(u_{k+1}^n, \tilde{F}_{k+1}^n, \tilde{\lambda}^n) \cdot x = 0$

CONTINUATION METHODS

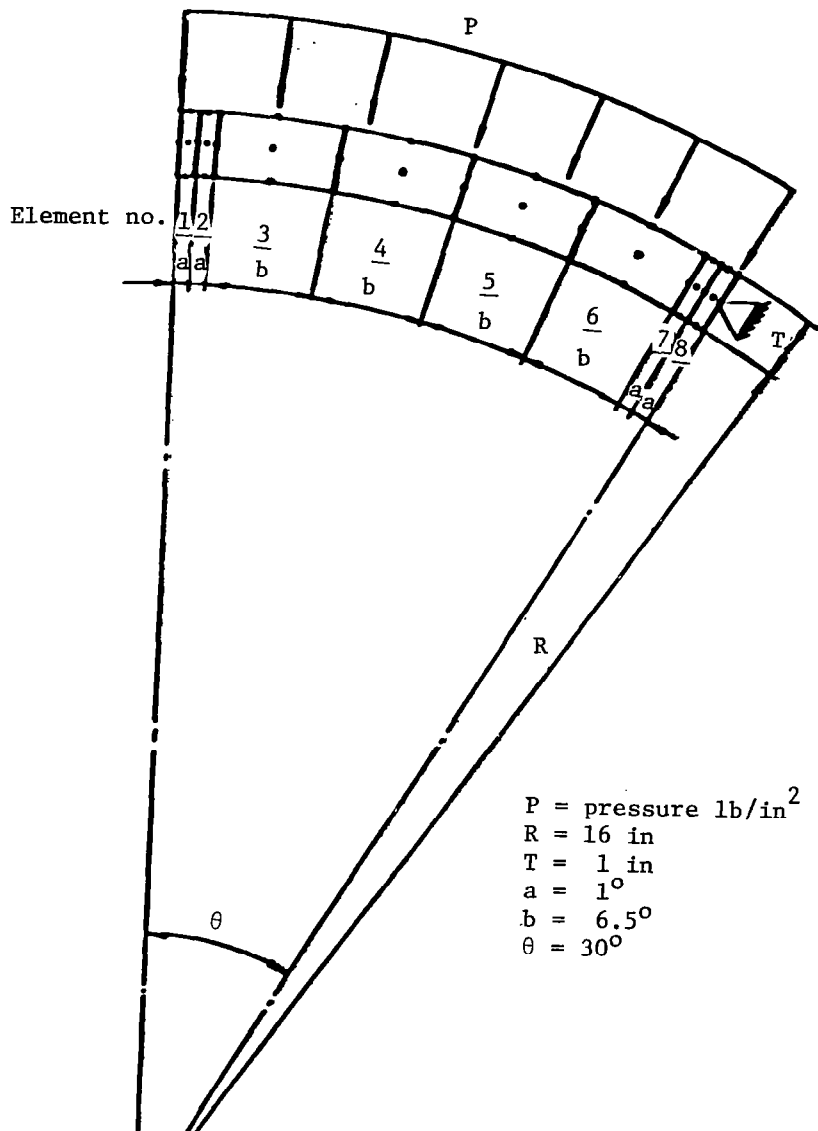
$$f(\tilde{x}(s), p(s)) = 0$$

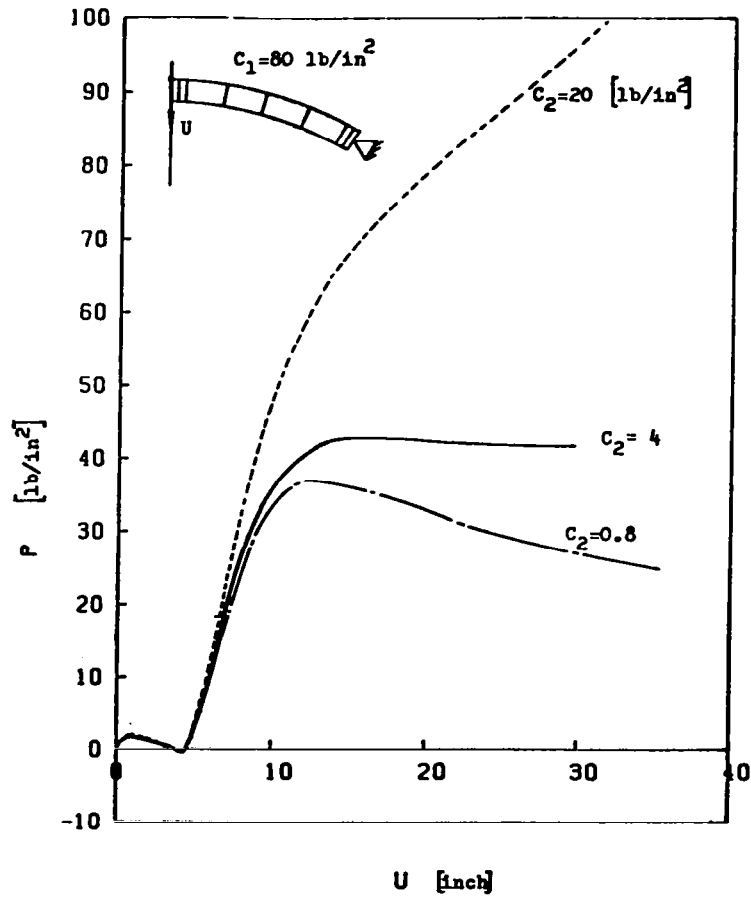
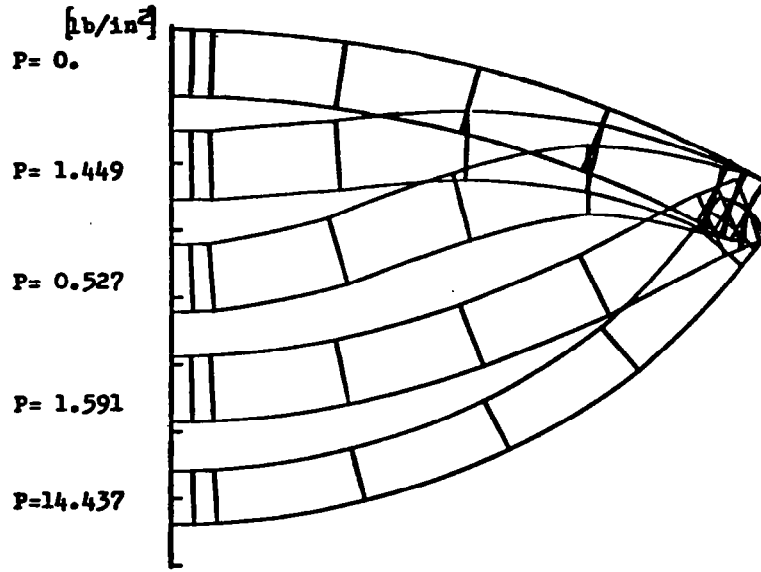
$$\dot{\tilde{x}}(s) \cdot \dot{\tilde{x}}(s) + \dot{p}^2(s) = 1 \iff N(\dot{\tilde{x}}, \dot{p}) = 0$$

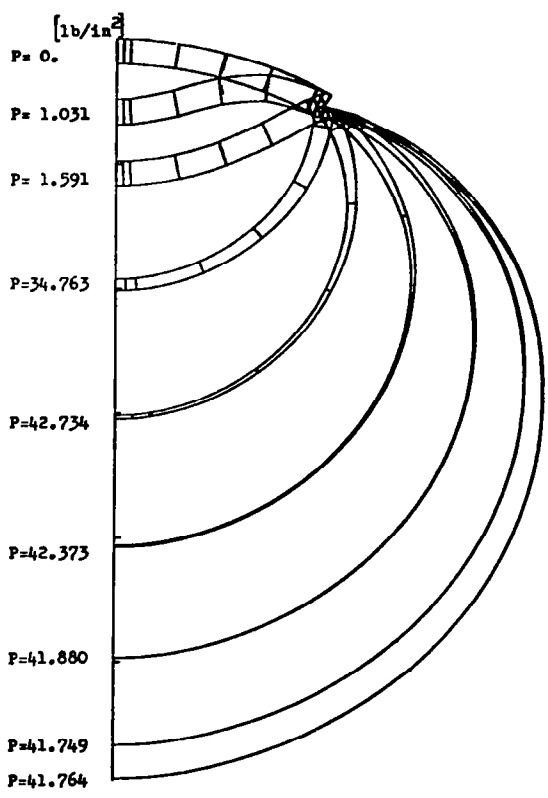
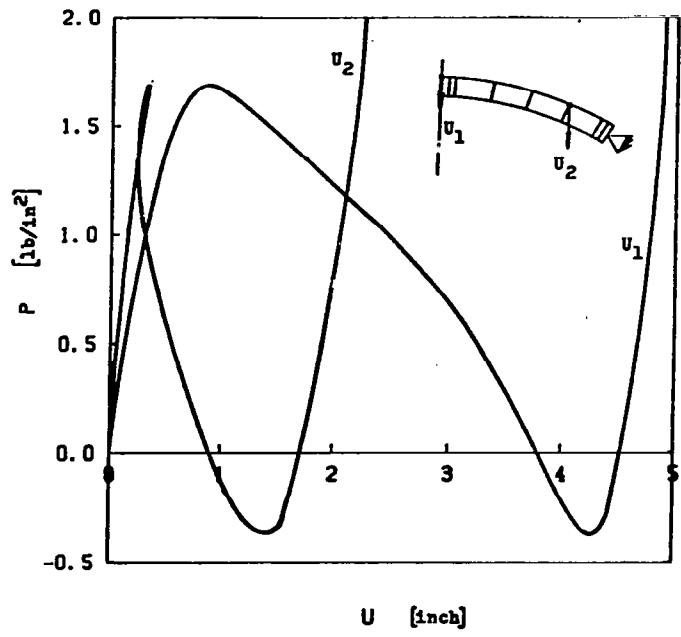


NUMERICAL EXAMPLES

Consider the inflation of a thick rubber spherical shell subjected to external loading. The shell is pressurized until it snaps through. Pressure continues to increase until the shell inflates. The material is assumed to be an incompressible Mooney-Rivlin material. The numerically stable Q2/P1 element is employed. Good results are obtained using the Riks-Crisfield method (refs. 5 and 7) with Newton-Raphson correction. Geometry of the shell is shown below and this is followed by several figures which illustrate numerical results. It is noted that the stiffness of the shell is strongly dependent on the material properties. In particular, for a fixed value of the Mooney-Rivlin constant C_1 , if C_2 is chosen sufficiently small, a limit point type behavior occurs in the inflated shell. This represents the phenomenon of a large decrease in pressure in an inflated balloon with a large increase in strain at the crown. This limit point behavior disappears for larger values of C_2 . (See ref. 11.)



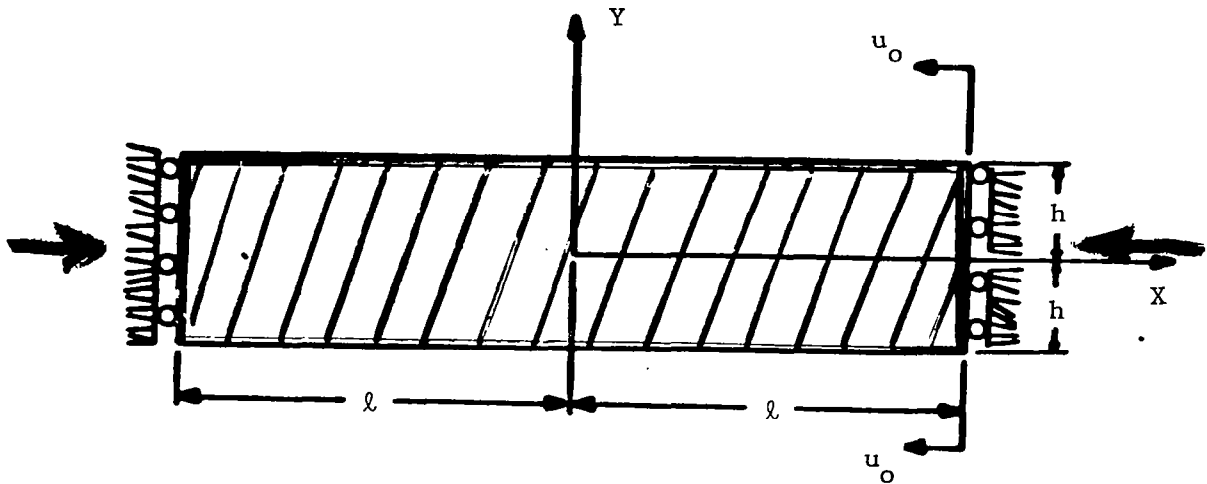




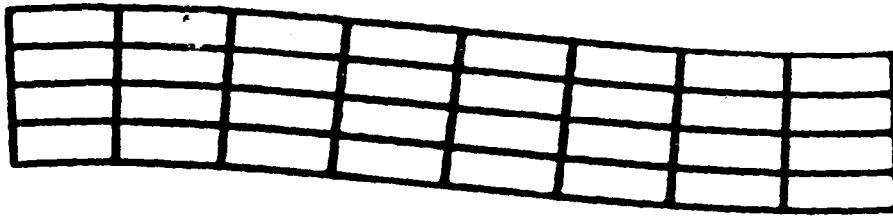
CALCULATION OF BIFURCATION PATHS

The Riks method (ref. 5) makes it possible to calculate bifurcation paths as well. A second example involves the buckling of a thick rubber plate under end thrust. This problem was analyzed by Sawyers and Rivlin (ref. 12), and provides a good example to test the bifurcation capabilities of the code. For low initial aspect ratios, a barreling mode of bifurcation is obtained, whereas for thinner slabs a flexural mode is obtained. The following figures show computed numerical results for these elements. Bifurcation branches were calculated for this problem as well. The following figures show the results of these calculations. After checking the energy of the system on each branch, the branch of lower energy is then calculated. In the first figure, branch one has lowest energy and branch two indicates a secondary bifurcation. The lower branches in each of the subsequent figures also represent lower energy equilibrium states. (See ref. 13.)

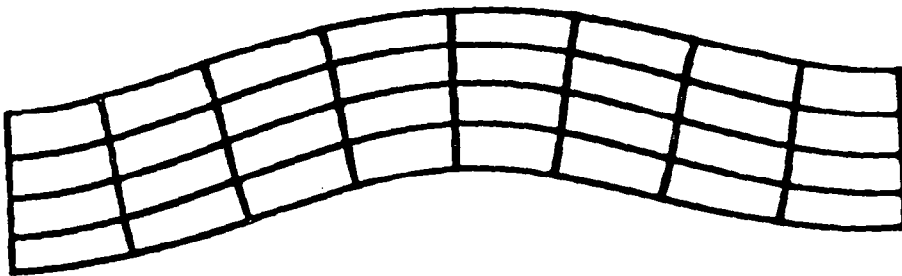
PLATE UNDER END THRUST



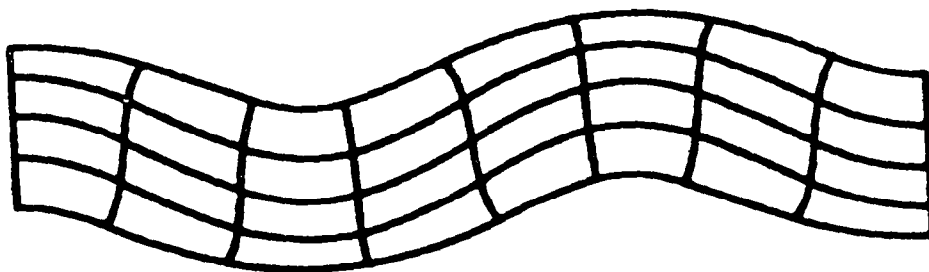
FIRST THREE BUCKLING MODES FOR A PLATE UNDER END THRUST



$$\lambda_x = 0.973$$



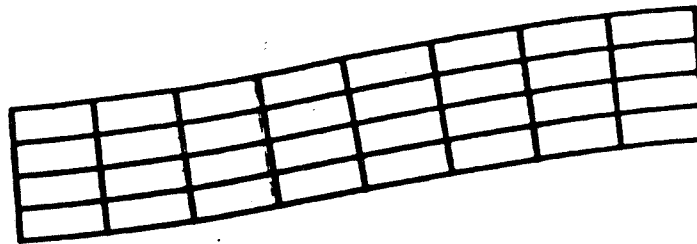
$$\lambda_x = 0.892$$



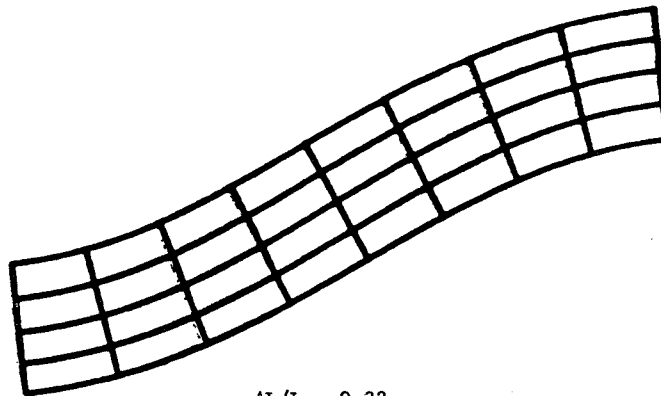
$$\lambda_x = 0.762$$

ORIGINAL PAGE IS
OF POOR QUALITY

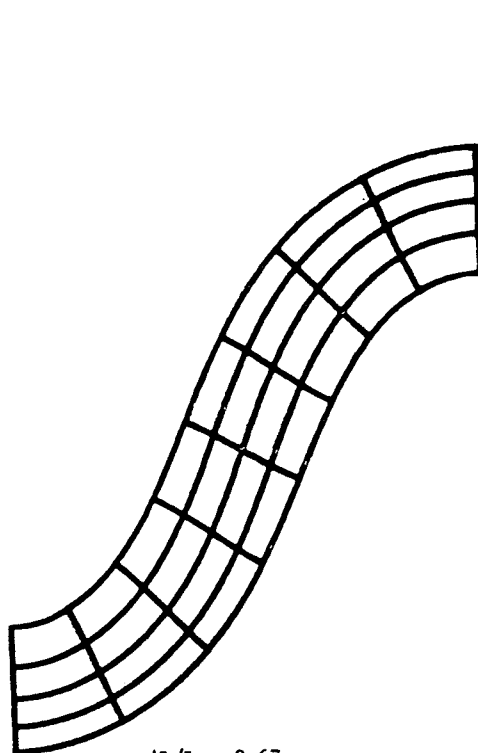
BUCKLED CONFIGURATIONS OF A PLATE FOR FIRST MODE BUCKLING



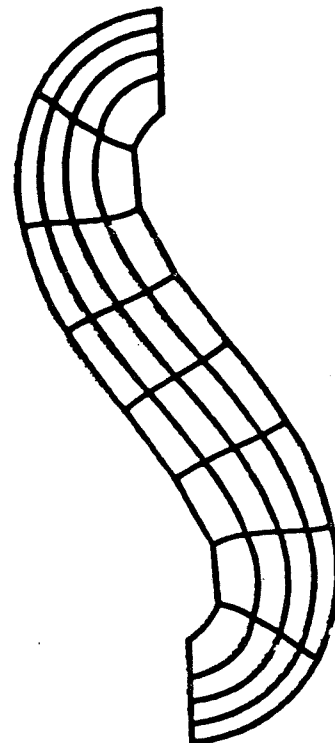
$$\Delta L/L = 0.30$$



$$\Delta L/L = 0.32$$

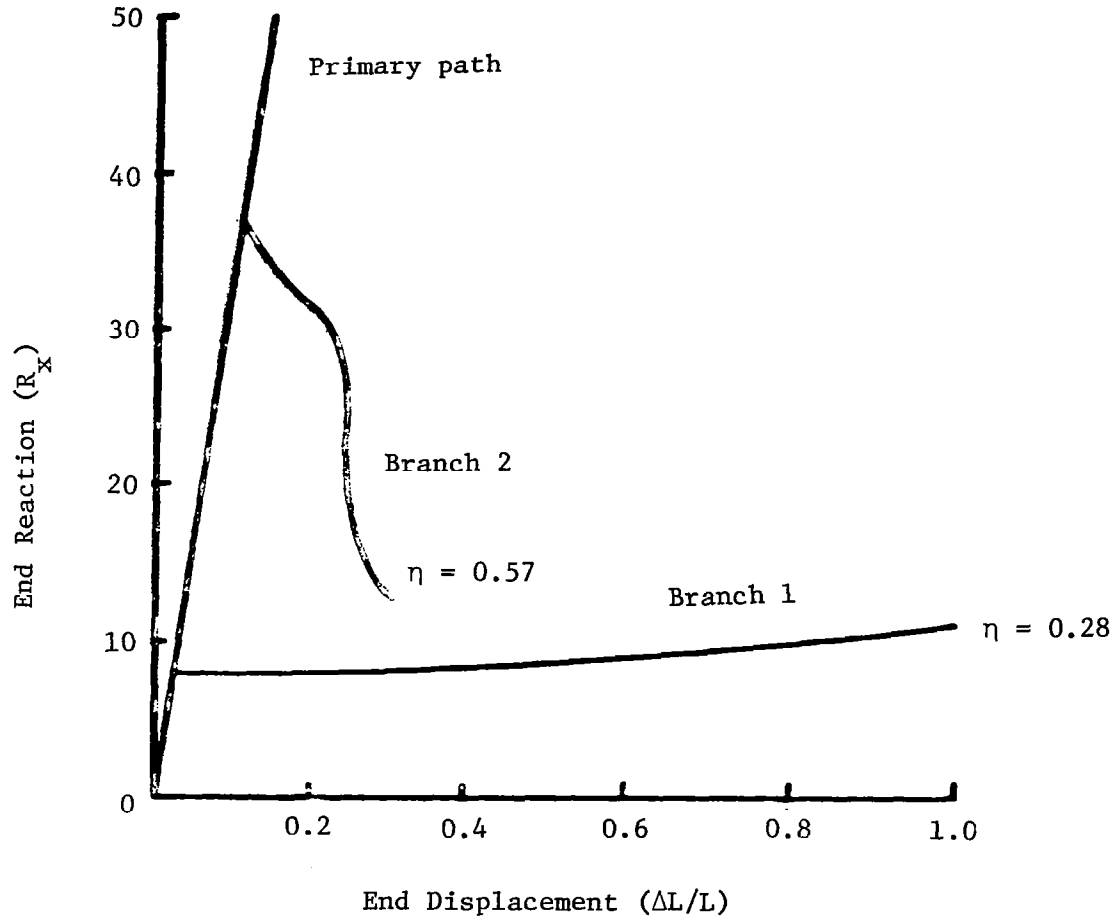


$$\Delta L/L = 0.67$$



$$\Delta L/L = 1.02$$

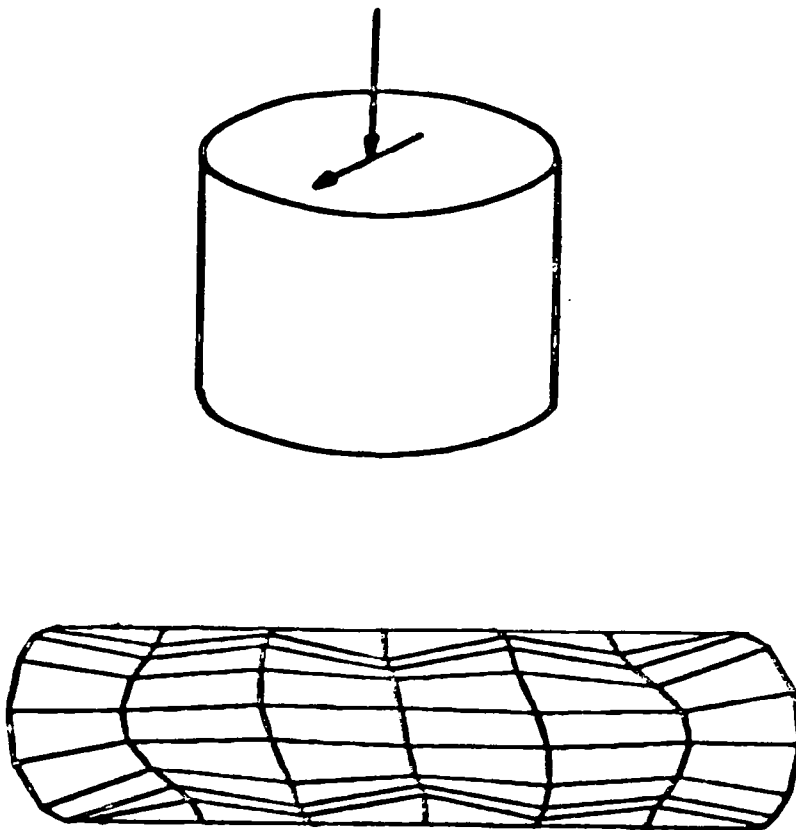
LOAD-DEFLECTION CURVE FOR A PLATE
ASPECT RATIO OF 0.18



COMPUTATIONAL PROBLEMS DURING HIGH COMPRESSION

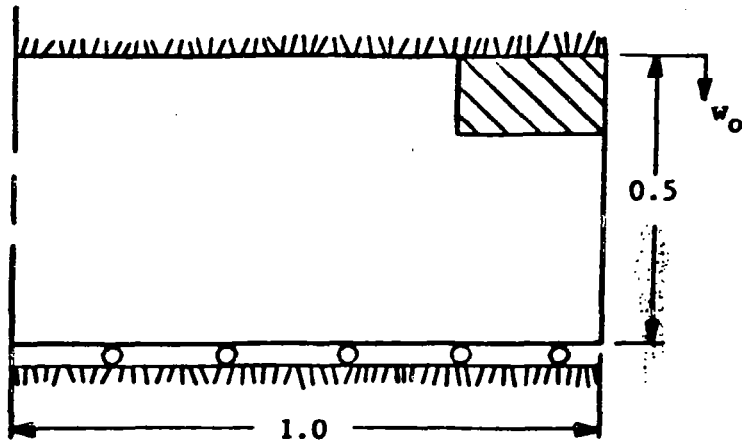
The augmented Lagrange method failed for problems with high compression as indicated in the figure below. An oscillatory mode was obtained at compressions of 30%. Here the $Q1/P0$ element was employed. In view of this, the continuation techniques with $Q2/P1$ elements were attempted in the following examples.

30% COMPRESSION

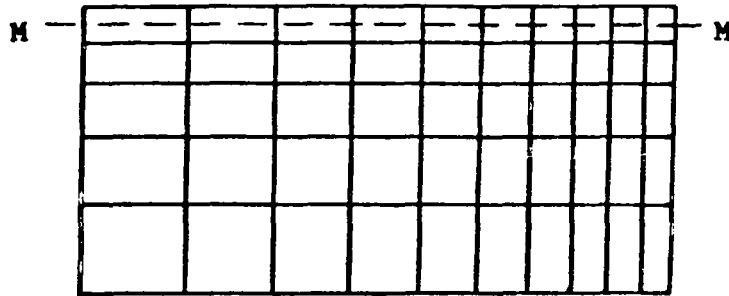


FIXED END CYLINDER

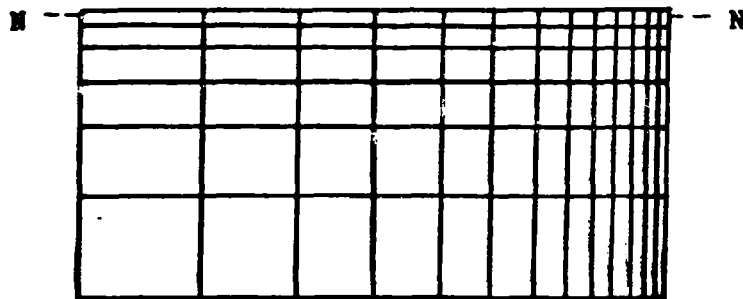
Area shown in deformation plots



Physical problem

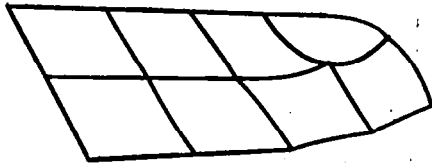


50-element mesh

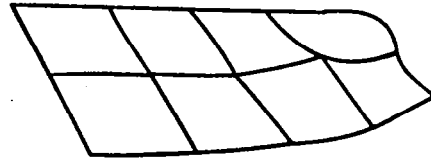


78-element mesh

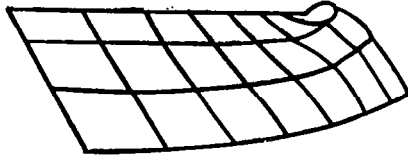
DISPLACED CONFIGURATION OF FIXED END CYLINDER: EIGHT-NODE ELEMENTS



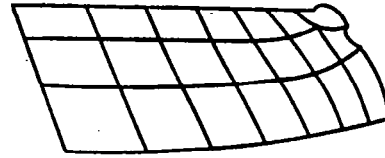
Q8DP, 50-element model, $w_0 = 0.1$



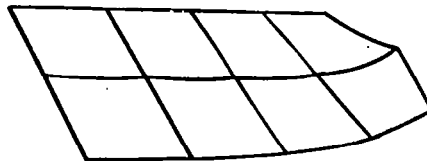
Q8CP, 50-element model, $w_0 = 0.1$



Q8DP, 78-element model, $w_0 = 0.1$

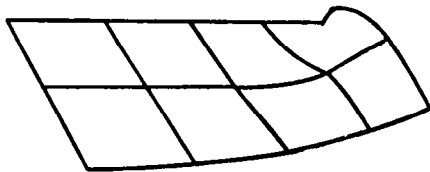


Q8CP, 78-element model, $w_0 = 0.1$

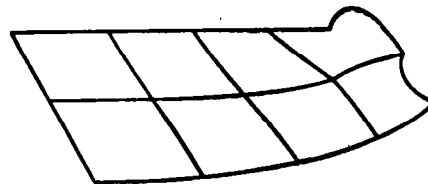


Q8D, 50-element model, $w_0 = 0.1$

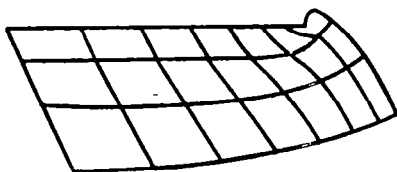
DISPLACED CONFIGURATION OF FIXED END CYLINDER: NINE-NODE ELEMENTS



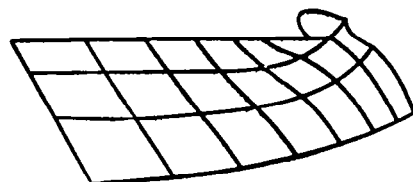
Q9DP, 50-element model, $w_0 = 0.1$



Q9CP, 50-element model, $w_0 = 0.1$



Q9DP, 78-element model, $w_0 = 0.1$

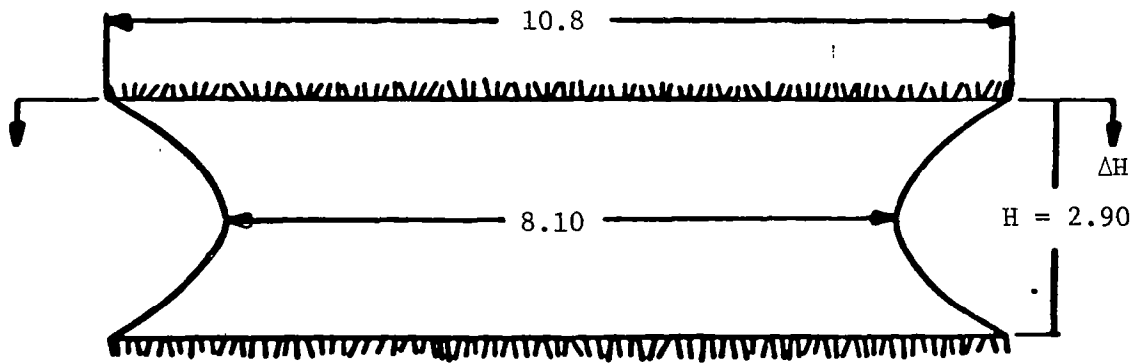


Q9CP, 78-element model, $w_0 = 0.1$

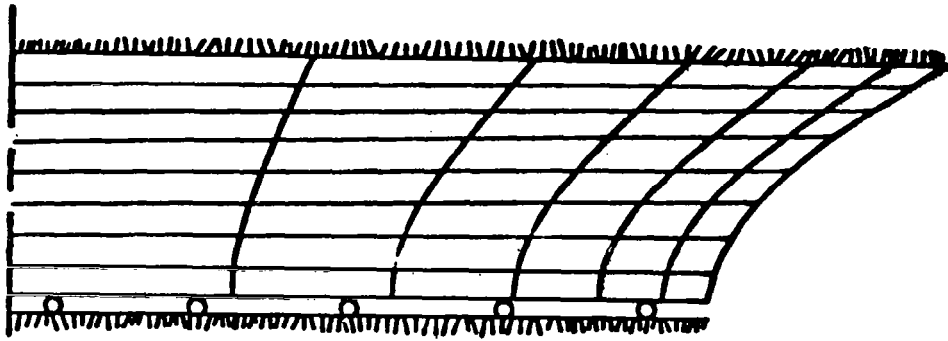
COMPRESSION OF A RUBBER BLOCK

Here a rubber block of revolution is one-quarter of the cross section of a block of revolution is shown. The block is subject to compression by uniform displacement of the edges. A strong singularity is developed in the free edge leading to a cusp as indicated in the calculated deformed configurations. Ultimately, contact of these surrounding regions occurs. This is a very difficult class of elastostatic problems and contact conditions must be incorporated in the analysis procedure to handle these problems.

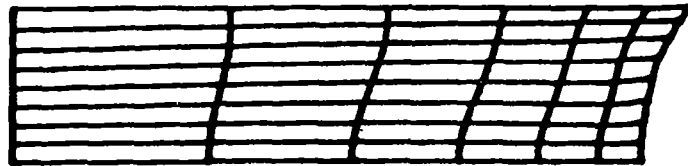
PLANE STRAIN BLOCK



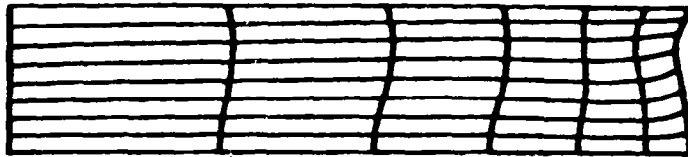
SYMMETRIC MODEL OF PLANE STRAIN BLOCK



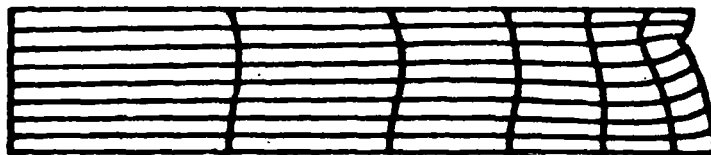
DEFORMATION BEFORE LIMIT POINT



$$\Delta H/H = 0.1175$$

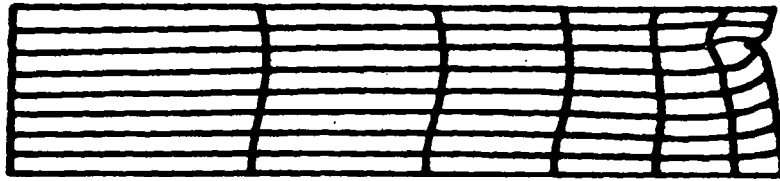


$$\Delta H/H = 0.1564$$

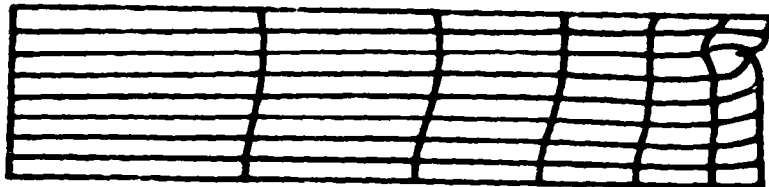


$$\Delta H/H = 0.1743$$

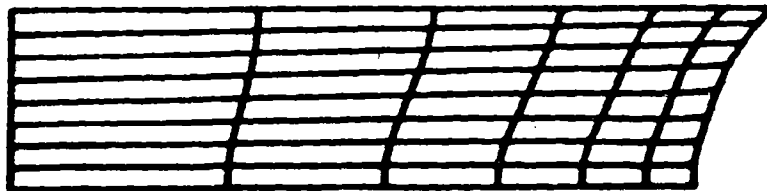
DEFORMATION AFTER THE LIMIT POINT



$$\Delta H/H = 0.164$$

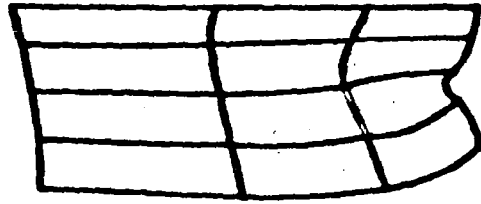


$$\Delta H/H = 0.151$$

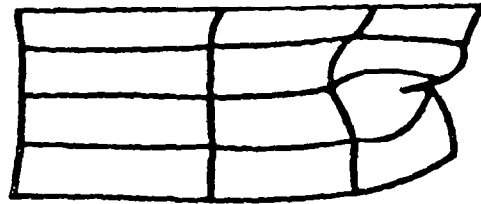


$$\Delta H/H = 0.104$$

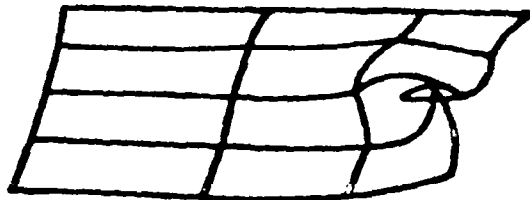
ENLARGED VIEW OF DEFORMED CONFIGURATION



At limit point

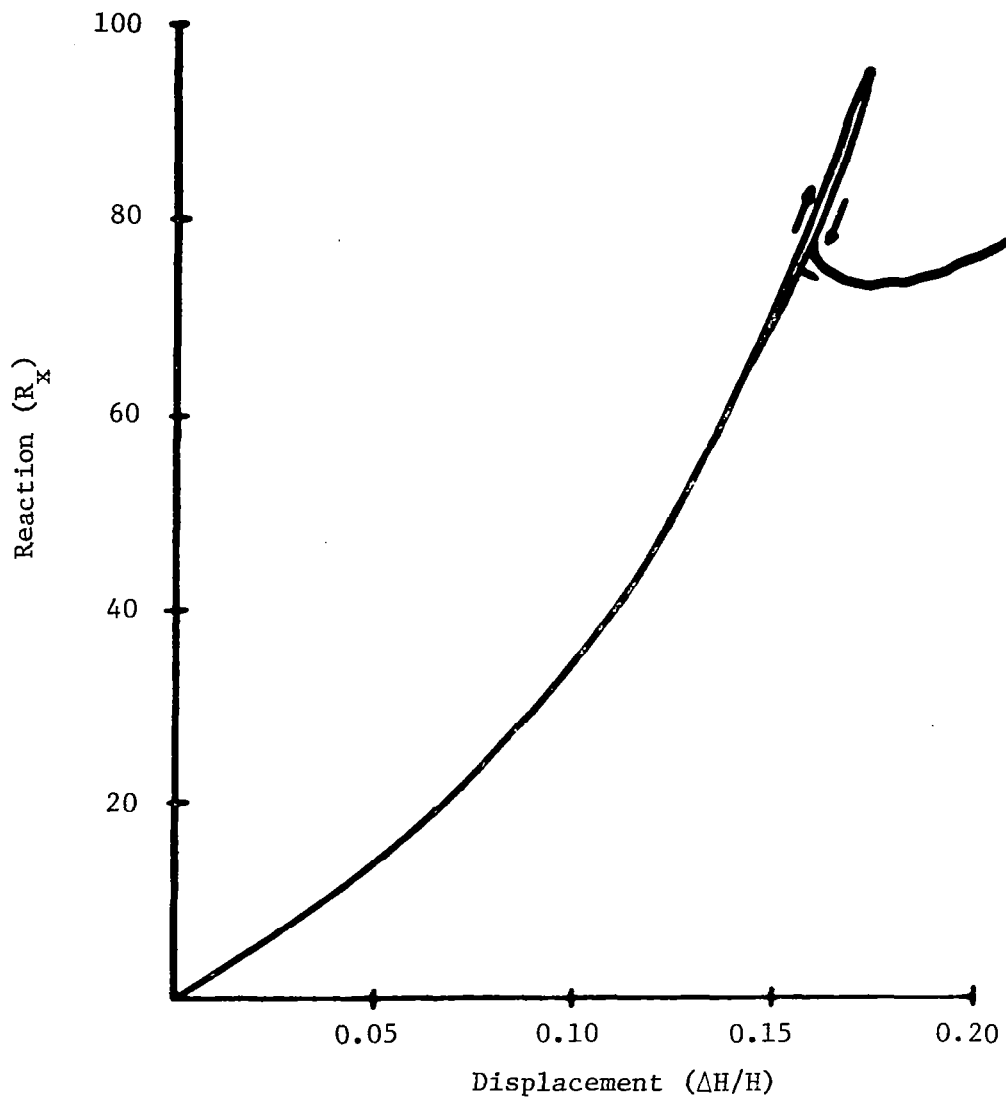


After limit point



Element boundary overlap at the cusp

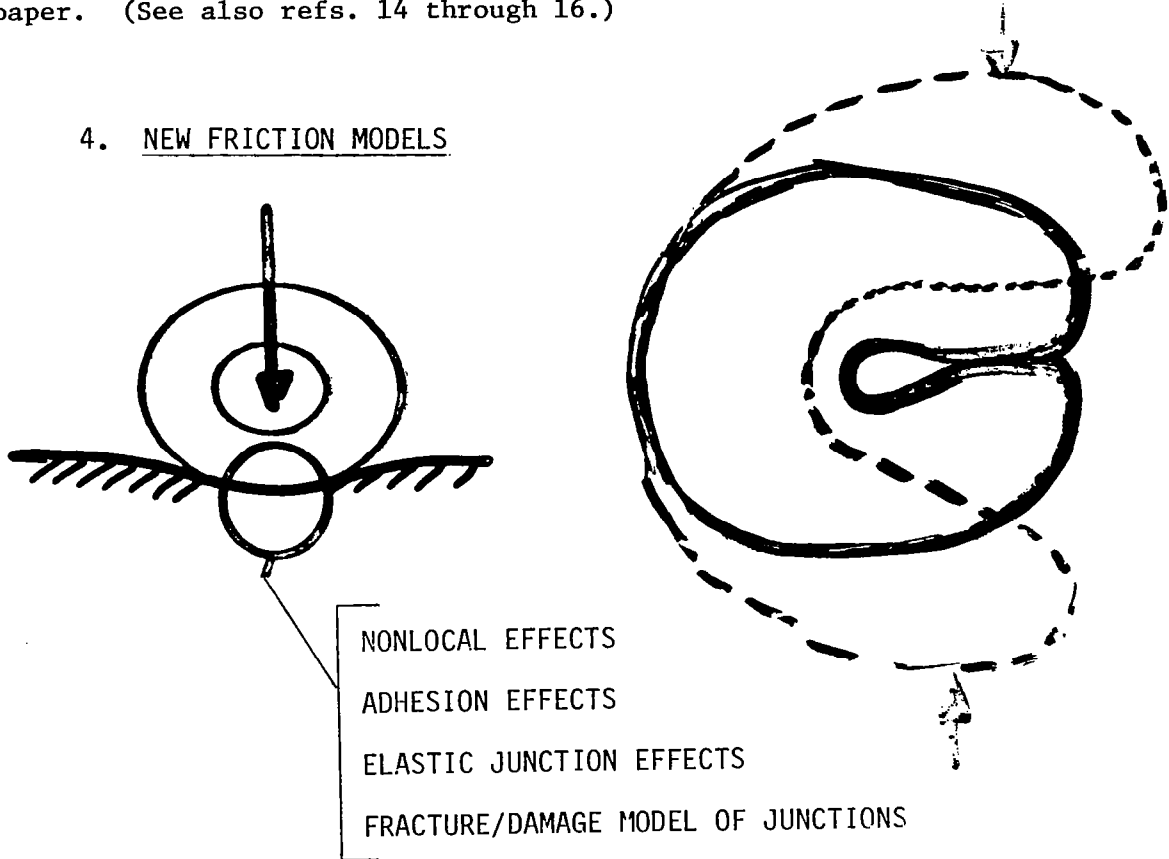
LOAD-DEFLECTION CURVE FOR THE PLANE STRAIN BLOCK



NEW FRICTION MODELS

It is now the generally held view that the classical Mohr-Coloumb law of friction is inadequate on both physical and mathematical grounds when modelling friction effects in real materials. For this reason, a preliminary study of several new non-classical friction laws have been undertaken. These friction laws include nonlocal effects to approximate deformed asperities, adhesion effects, and elastic junction effects, and ultimately will include fracture and damage models of the junctions on the contact surface. The general form of these contact laws is given below, where σ_T is the tangential frictional stress, ν is the coefficient of friction, which may depend upon the number of loading cycles and the stress state on the contact surface, gradients of deformation, etc., S_ρ is a smoothing operator with ρ representing a characteristic dimension of deformed asperities on the contact surface, σ_n is the normal contact pressure, and ϕ_ϵ represents a compliance function which models the elasticity and elastoplasticity of interface junctions. This compliance reaction is given as an anti-symmetric function of the value of the tangential velocity vector \dot{u}_T on the contact surface. An algorithm has been developed for implementing this new friction law. Some preliminary results are indicated in the final two figures of this paper. (See also refs. 14 through 16.)

4. NEW FRICTION MODELS



$$\sigma_T(\underline{u}) = \nu(\nabla \underline{u}, t) S_\rho(\sigma_N(\underline{u})) \phi_\epsilon(\|\dot{\underline{u}}_T\|)$$

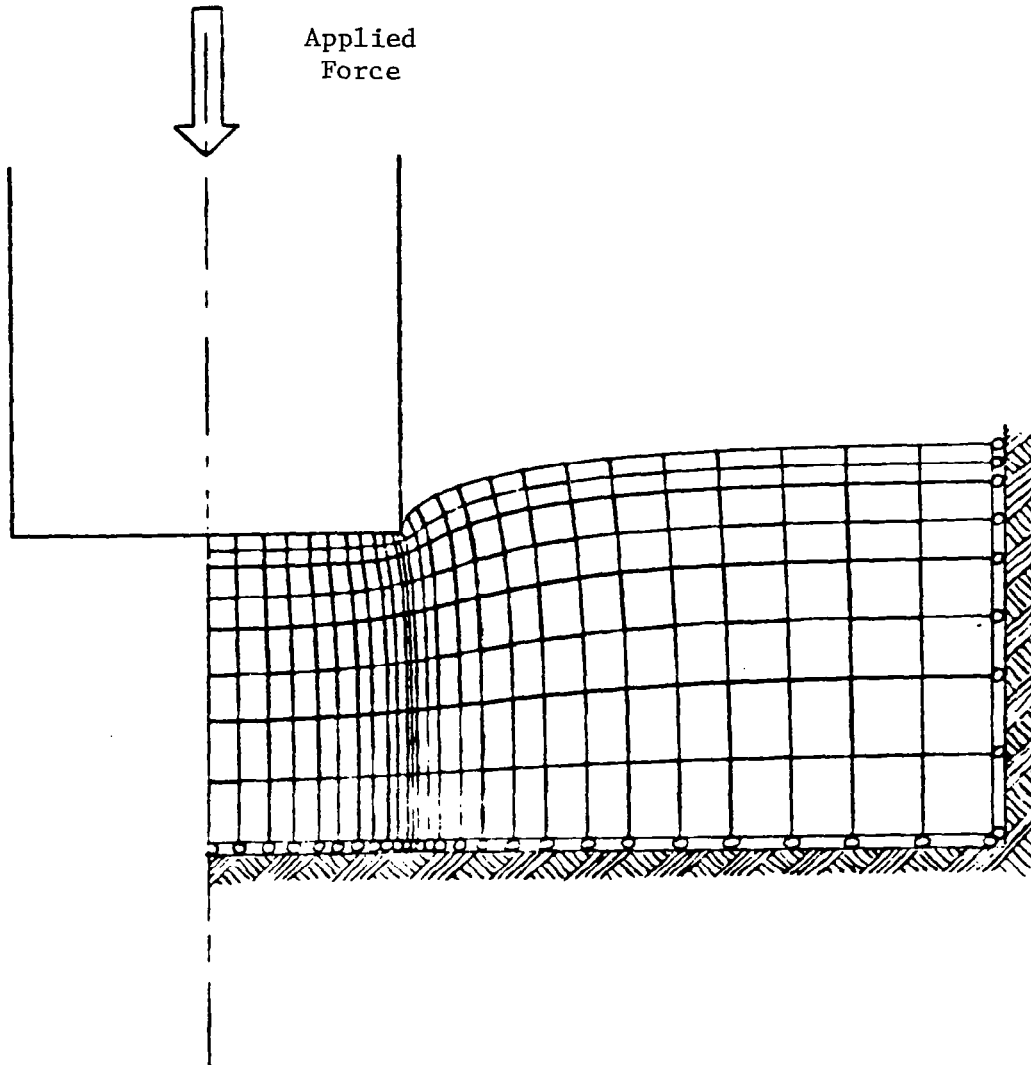
CYCLIC/DAMAGE

NONLOCAL

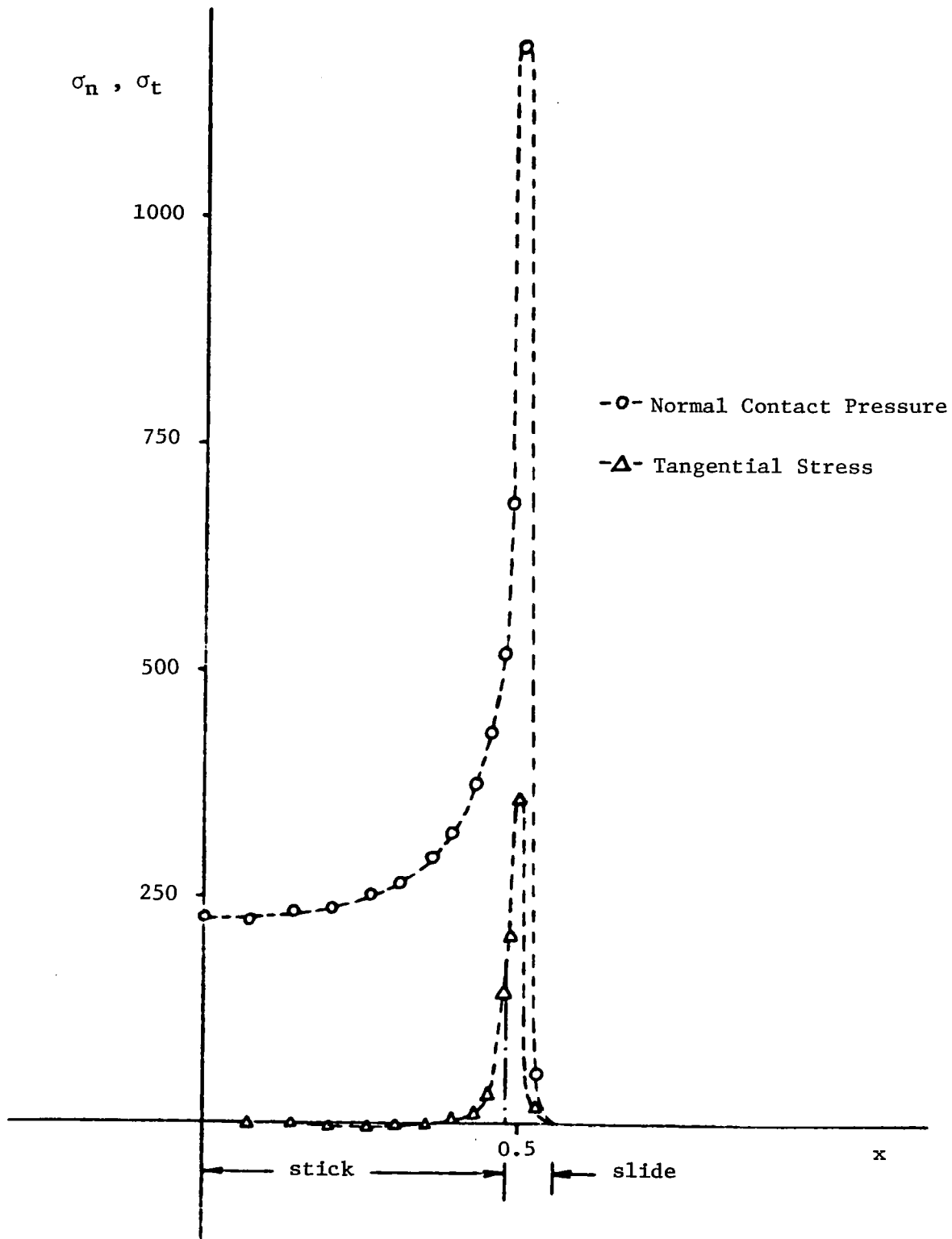
JUNCTION ELASTICITY & PLASTICITY

NEW FRICTION MODEL APPLICATIONS

An example of the indentation of a rigid cylindrical stamp into an elastic slab is considered. A non-classical friction law is used, with $\rho = -0.1$, $\epsilon = 10^{-4}$, $E = 1000$, $\mu = 0.6$. Nine-node bi-quadratic elements were used. Deformed shape and stresses on the contact surface are shown.



NEW FRICTION MODEL APPLICATIONS (concluded)



REFERENCES

1. Glowinski, R.; Lions, J. L.; and Tremolieres, R.: *Analyse Numerique des Inequations Variationnelles*. Dunod-Bordas: Paris, 1976.
2. Oden, J. T.: *Penalty Methods for Constrained Problems in Nonlinear Elasticity*. IUTAM Symposium on Finite Elasticity, Martinum-Nijhoff Publ.: The Hague, 1982, pp. 281-300.
3. LeTallec, P.; and Oden, J. T.: *Existence and Characterization of Hydrostatic Pressure in Finite Deformations of Incompressible Elastic Bodies*. *J. Elast.*, vol. 11, no. 4, 1981, pp. 341-357.
4. Oden, J. T.; and Jacquotte, O.: *Stability of RIP Methods for Stokesian Flows*. TICOM Report No. 82-2, Texas Institute for Computational Mechanics, Austin, 1982.
5. Riks, E.: *The Application of Newton's Method to the Problems of Elastic Stability*. *J. Appl. Mech.*, vol. 39, 1972, pp. 1060-1066.
6. Keller, H. B.: *Practical Procedures in Path Following Near Limit Point*. *Computational Methods in Applied Sciences and Engineering*, R. Glowinski and J. L. Lions, eds., North-Holland, 1982.
7. Crisfield, M. A.: *A First Incremental/Iterative Solution Procedure That Handles 'Snap-Through'*. *Computers and Structures*, vol. 13, 1981, pp. 55-62.
8. Padovan, J.; and Arechaga, T.: *Formal Convergence Characteristics of Elliptically Constrained Incremental Newton-Raphson Algorithms*. *Int. J. Engn. Sci.*, vol. 20, no. 10, 1982, pp. 1077-1097.
9. Wempner, G. A.: *Discrete Approximations Related to Nonlinear Theories of Solids*. *Int. J. Solids Structures*, vol. 7, 1971, pp. 1581-1599.
10. Rheinboldt, W. C.: *Numerical Analysis of Continuation Methods for Nonlinear Structural Problems*. *Computers and Structures*, vol. 13, 1981, pp. 103-113.
11. Oden, J. T.: *Finite Elements of Nonlinear Continua*. McGraw-Hill, 1972.
12. Sawyers, K. N.; and Rivlin, R. S.: *Stability of a Thick Elastic Plate Under Thrust*. *J. Elast.*, vol. 12, 1980, pp. 101-125.
13. Miller, T. H.: *A Finite Element Study of Instabilities in Rubber Elasticity*. Ph.D. Dissertation, Univ. of Texas, Austin, 1982.
14. Pires, E. B.: *Analysis of Nonclassical Friction Laws for Contact Problems in Elastostatics*. Ph.D. Dissertation, Univ. of Texas, Austin, 1982.
15. Oden, J. T.; and Pires, E. B.: *Nonlocal and Nonlinear Friction Laws and Variational Principles for Contact Problems in Elasticity*. *J. Appl. Mech.*, 1983, in press.
16. Oden, J. T.; and Pires, E. B.: *Numerical Analysis of Certain Contact Problems in Elasticity With Nonclassical Friction Laws*. *Computers and Structures*, vol. 16, no. 1-4, 1982, pp. 481-485.